International Journal of Coal Science & Technology (2023) 10:18
https://doi.org/10.1007/s40789-023-00579-4

RESEARCH

Slope stability prediction based on a long short-term memory neural network: comparisons with convolutional neural networks, support vector machines and random forest models

Faming Huang[1] · Haowen Xiong[1] · Shixuan Chen[1] · Zhitao Lv[1] · Jinsong Huang[2] · Zhilu Chang[1] · Filippo Catani[3]

Received: 24 July 2022 / Accepted: 1 March 2023

Abstract
The numerical simulation and slope stability prediction are the focus of slope disaster research. Recently, machine learning models are commonly used in the slope stability prediction. However, these machine learning models have some problems, such as poor nonlinear performance, local optimum and incomplete factors feature extraction. These issues can affect the accuracy of slope stability prediction. Therefore, a deep learning algorithm called Long short-term memory (LSTM) has been innovatively proposed to predict slope stability. Taking the Ganzhou City in China as the study area, the landslide inventory and their characteristics of geotechnical parameters, slope height and slope angle are analyzed. Based on these characteristics, typical soil slopes are constructed using the Geo-Studio software. Five control factors affecting slope stability, including slope height, slope angle, internal friction angle, cohesion and volumetric weight, are selected to form different slope and construct model input variables. Then, the limit equilibrium method is used to calculate the stability coefficients of these typical soil slopes under different control factors. Each slope stability coefficient and its corresponding control factors is a slope sample. As a result, a total of 2160 training samples and 450 testing samples are constructed. These sample sets are imported into LSTM for modelling and compared with the support vector machine (SVM), random forest (RF) and convolutional neural network (CNN). The results show that the LSTM overcomes the problem that the commonly used machine learning models have difficulty extracting global features. Furthermore, LSTM has a better prediction performance for slope stability compared to SVM, RF and CNN models.

Keywords Slope stability prediction · Long short-term memory · Deep learning · Geo-Studio software · Machine learning model

1 Introduction

The mechanical balance of slopes is often destroyed due to natural or man-made factors, which induces landslides and other geological disasters and further causes casualties and economic losses (Palenzuela Baena et al. 2019; Chang et al. 2022). Accurately predicting landslides allows for promptly transferring personnel and property and minimizing losses (Huang et al. 2016; Li et al. 2021). Therefore, it is very important to predict slope stability quickly and accurately.

The occurrence of landslides is a long-term process, which is nonlinear and complex from a gradual evolution to sudden macroscopic slope slippage (Kumar and Basudhar 2018; Criss et al. 2020; Jiang et al. 2022). Due to the complexity of the structure and discontinuity of the physical and mechanical properties of slope mass, as well as the variability and effectiveness of control factors acting on the slope, slope engineering can be regarded as an uncertain, nonlinear, dynamic and open complex system in which the stability is comprehensively affected by geological and engineering factors (Bui et al. 2019; Dai et al. 2021; He et al. 2021; Wu et al. 2022). Most of these control factors have the characteristics of randomness, ambiguity, variability and other

✉ Zhitao Lv
lvzhitao@ncu.edu.cn

[1] School of Civil Engineering and Architecture, Nanchang University, Nanchang 330031, China

[2] Discipline of Civil, Surveying and Environmental Engineering, Priority Research Centre for Geotechnical Science and Engineering, University of Newcastle, Callaghan, NSW 2287, Australia

[3] Department of Geosciences, University of Padova, Padua, Italy

Published online: 10 April 2023

uncertainties. Their influence weights on slope stability vary, and there are complex nonlinear relationships between these control factors (Kang et al. 2017).

Many methods were proposed for a slope stability calculation, among which the limit equilibrium method and numerical simulation method were the two most widely used method (Yang et al. 2020). Both methods have their advantages and disadvantages. For the limit equilibrium method, it is very difficult to find the critical slip surface because there are many potential slip surfaces (Yang et al. 2019b). For the numerical simulation method, the selection of constitutive models, mechanical parameters and boundary conditions significantly affect its accuracy, and it often requires rich engineering experience and on-site back analysis to make a rational selection and acquire reasonable results (Qi and Tang 2018; Ray et al. 2020). Moreover, it generally takes a long time to establish a computer model and perform analysis for numerical simulation methods (Abdalla et al. 2014). Therefore, there are still considerable challenges in predicting slope stability.

In recent years, machine learning models have attracted an attention in solving these highly complex, nonlinear, and multi-variable geotechnical issues. Researchers attempt to use the artificial neural networks (ANNs), support vector machine (SVM) algorithms and other methods to solve such issues (Rukhaiyar et al. 2017; Huang et al. 2020a). The ANNs have shown a high degree of success in function approximation in different fields including geotechnical engineering. An ANN is a computer model with a structure that naturally imitates the information processing and optimization strategy of human brain (Zhang and Goh 2016). Through weighted connections, the input variables stored in the input layer neurons are redistributed to hidden neurons and then transformed into the neural network response in the output layer neurons (Selvaraju et al. 2020). Researchers have proposed various ANN models for calculating slope stability. For example, Qian et al. (2019) proposed a slope stability evaluation tool based on the ANN model. Gao et al. (2019) proposed to use the ANN model optimized by the imperialist competition algorithm to solve the slope stability problem.

Deep learning model is a new branch of machine learning developed in recent years and is considered an extension of neural networks. Structurally, it is different from previous machine learning models in that it has more and deeper network layers. Algorithmically, it can automatically extract features instead of manually designing features as in traditional machine learning (Schmidhuber 2015; Huang et al. 2022b). Artificial design features have some shortcomings. First, the design is difficult and requires constant trial because of error. Second, different features need to be designed for different problems (Yao et al. 2017). On facial recognition detection datasets, the deep learning accuracy can be as high as 99.47%, which is much higher than 60% of the traditional face recognition algorithm *eigenface* because automatically selected features are more accurate than manually designed features (Wu et al. 2019). The "deep" network structure of deep learning can express information hierarchically. The idea is to stack multiple layers; the output of the upper layer is used as an input of the next layer, and different features are extracted from different layers to achieve the layered expression of features (Zhou 2018). Moreover, deep learning extracts global features instead of local features. Therefore, it is more fault tolerant. Even if some local areas are missing, correct results can still be obtained based on other global features, avoiding the classification errors caused by local areas (Liang et al. 2017; Huang et al. 2020b). Shallow machine learning is less fault tolerant because it is difficult to extract global features and cannot make a full use of the contextual information. Thus, the deep learning is more capable of expressing object characteristics than the traditional machine learning. Based on the advantages of deep learning, some scholars have applied deep learning to slope engineering. For example, Wang et al. (2020b) applied deep learning to rock classification to facilitate further study of slope stability. Tan et al. (2021) made a rapid assessment of landslide risk grade based on deep learning, which accelerated the landslide risk grade determination process.

The Long short-term memory (LSTM) neural network is a new deep learning algorithm developed in recent years, which has great advantages in processing dynamically changing data (Zhao et al. 2020). The LSTM is essentially a recurrent neural network having a long-term dependence problem. That is, when learning a long sequence, the recurrent neural network shows gradient disappearance and gradient explosion and cannot determine the nonlinear relationship of a long time span (Wang et al. 2018). The LSTM model is proposed to solve this problem. In the LSTM, the "gate" structure protects and controls the unit state and selectively allows information to pass through, which can effectively solve the recurrent neural network gradient disappearance and gradient explosion problem. Recently, researchers have applied the LSTM to other fields. For example, Chen et al. (2021) predicted China's particulate pollution based on the LSTM, and the results showed that the model has a high prediction accuracy. Liu et al. (2018) proposed a wind speed prediction model based on the LSTM, which achieved a good prediction performance. However, the LSTM model has not been used in slope stability prediction.

In this study, LSTM is applied to landslide stability prediction. Five control factors representing most slope properties including the slope height, slope angle, internal friction angle, cohesion and soil weight, are selected as input variables from landslide influencing factors. Within the value range of each variable, its value is selected according to the idea of interpolation, and the values of each variable are

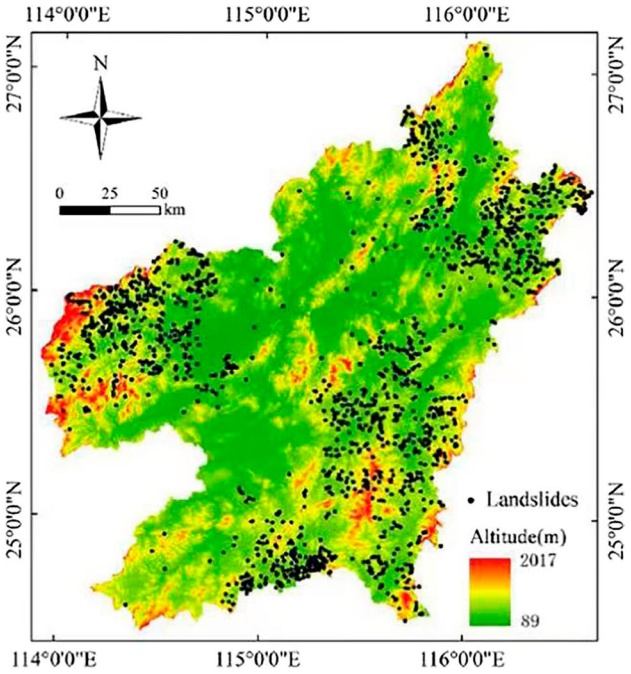

Fig. 1 Location of the study area and landslide inventory

combined to obtain different slope data. Typical soil slopes are established through the Geo-Studio software, and the "true value" of the slope stability factor of each slope is calculated. The obtained training dataset and prediction dataset are input into the LSTM model to predict slope stability. The SVM, random forest (RF) and convolutional neural network (CNN) are used as the comparison models. The prediction data obtained by the four models are compared and analyzed to explore the feasibility of LSTM in slope stability prediction.

2 Introduction of machine learning models

2.1 Modelling processes and ideas

First, the landslides inventory of Ganzhou City, Jiangxi province, from 1998 to 2010 was collected and analyzed to obtain the geometric properties of the slope soil material in this area (Fig. 1). By referring to the relevant literature, five control factors, including the slope height, slope angle, internal friction angle, cohesion and volumetric weight, were selected as input variables of the machine learning model, and the value range of each variable was determined (Zhang and Goh 2016; Gao et al. 2019; Qian et al. 2019; Selvaraju et al. 2020). Based on the interpolation method, the variable values were evaluated within their ranges, and the variable values were arranged and combined to obtain several groups of slope data. The obtained slope data were input into the Geo-Studio software, and the slope stability factor of the corresponding slope was calculated by the limit equilibrium method.

Each slope stability factor and its five corresponding control factors form a slope sample. A total of 2160 training samples and 450 testing samples were constructed in this study. Then, the slope stability prediction model based on machine learning was established. The fitting ability and prediction performance of these models were trained with training samples and the parameters in each prediction model were determined. Finally, the remaining slope sample was input to the trained model for a slope stability prediction. The slope stability factor of the predicted sample slope is output. The modelling process was shown in Fig. 2.

2.2 Introduction of machine learning models

In this study, four machine learning models, the LSTM, CNN, SVM and RF, were selected to predict slope stability (Sun et al. 2020; Huang et al. 2021). Among them, the LSTM model is the research object of this study with the other three models for comparisons to explore the feasibility of LSTM in slope stability prediction.

2.2.1 Long short-term memory model

The LSTM is a special recurrent neural network, which has great advantages in dealing with dynamically changing data (Fig. 3). The LSTM can effectively prevent the long-term dependence problems in the recurrent neural network, that is, the gradient explosion and gradient disappearance. Due to its memory block mechanism, it can be used to describe continuous output on the time state. The LSTM is applied to the regional dynamic landslide disaster prediction model. The information in this model can directly flow from one sample node to the next sample node (Xie et al. 2019).

All recurrent neural networks have the form of a chain of repeated neural network modules. In a standard recurrent neural network, these repeating modules have a very simple structure, such as a single tanh layer. Similarly, the LSTM also has this chain structure. However, the repeating LSTM module has a different structure. There is not only one neural network layer but four layers that interact in a very special way (Wang et al. 2020a).

The cell state is the key to the LSTM, and it extends along the horizontal line that runs through the top of the structure diagram. There are only some small linear interactions in the process and information can flow through this chain without changes. The LSTM can delete or add information to the cell state. These functions are carefully adjusted by a structure called "gate". The gate consists of a *sigmoid* neural network layer (σ) and a point-by-point multiplication operation, which can selectively allow information to pass through. The

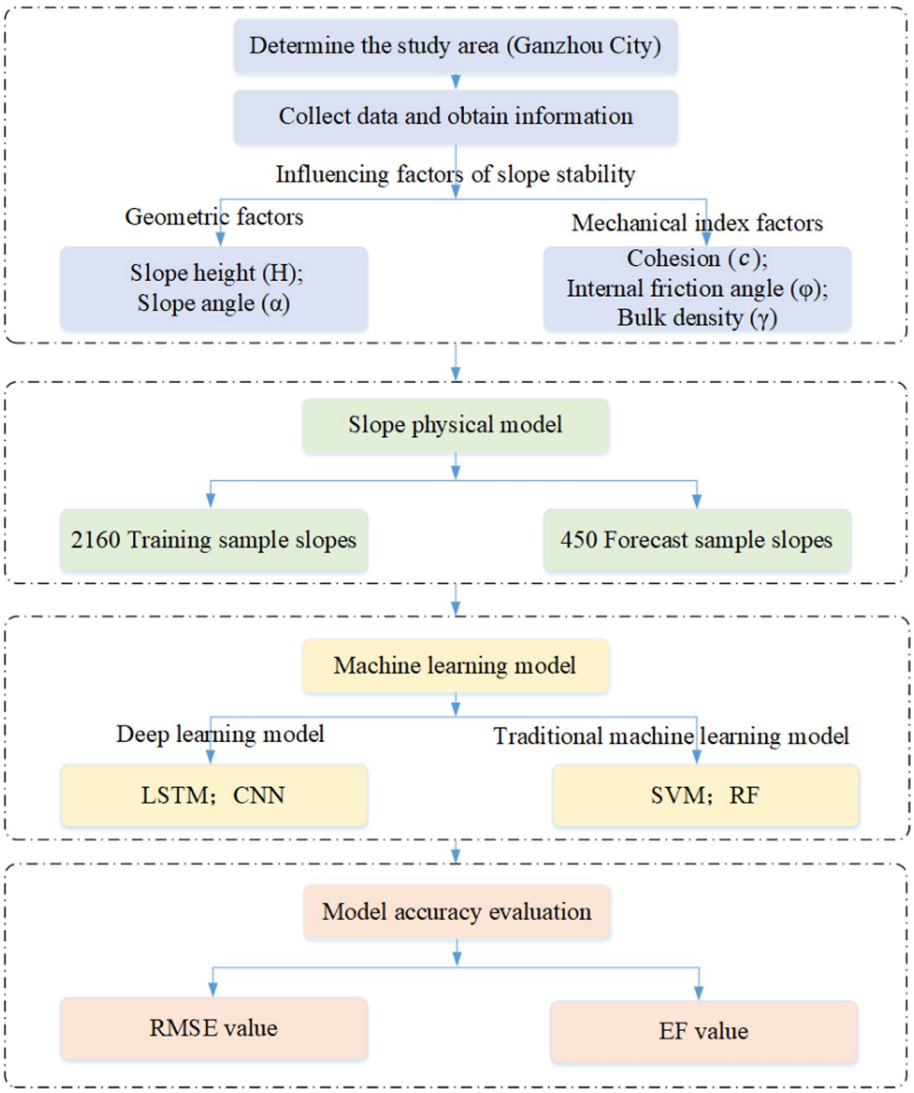

Fig. 2 Modeling flow chart

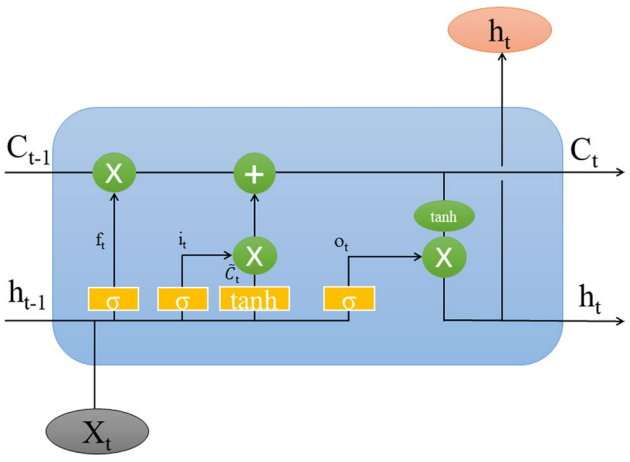

Fig. 3 Structure diagram of the LSTM model

sigmoid layer outputs a number between 0 and 1, describing whether each component is allowed to pass. When the value is 0, it means “do not let any content pass”, When the value is 1, it means "let all content pass". The expression of the *sigmoid* function is as:

$$sigmoid(x) = \frac{1}{1 + e^{-x}} \tag{1}$$

There are three such gates in the LSTM: the “forget gate”, the “input gate” and the “output gate”. These three gates are used to protect and control the unit state (Amin et al. 2019). Therefore, as a filter, each door has its job to achieve different purposes:

(1) The forget gate (f_t) filters the input information to determine which information to keep or forget. The forget gate looks at the input h_{t-1} and x_t through the *sigmoid* neural network layer and outputs a number between 0 and 1 for the information of c_{t-1} in a unit state, thereby determining whether the input information is retained or forgotten:

$$f_t = \sigma W_f \cdot [h_{t-1}, x_t] + b_f \tag{2}$$

where x_t is the input data at the current moment, h_{t-1} is the output of the hidden unit at the previous moment, W_f represents the weight matrix of the forget gate and b_f represents the offset.

(2) The input gate (i_t) continuously updates the transmitted information, filters out the information that needs to be retained, and updates the unit status at the moment. First, the *sigmoid* network layer of the input gate filters the input information. Next, the tanh layer creates a new vector $\tilde{c}_t$ and combines both i_t and $\tilde{c}_t$ to obtain a new candidate value c_t (Tian et al. 2018):

$$i_t = \sigma(W_i \cdot [h_{t-1}, x_t] + b_i) \tag{3}$$

$$\tilde{c}_t = \tanh(W_c \cdot [h_{t-1}, x_t] + b_c) \tag{4}$$

$$c_t = f_t \cdot c_{t-1} + i_t \cdot \tilde{c}_t \tag{5}$$

where c_t represents the cell state at time t, c_{t-1} represents the cell state at time t-1, W_i and W_c represent the weight matrix, b_i and b_c represent the offset.

(3) The output gate (o_t) is a result of combining the forget gate and the input gate to determine the output of the current neural unit. The output data is used as an input to the next unit. The output gate determines which part of the unit state to output through the *sigmoid* neural network layer. Then, the value of the new cell state c_t is changed to between -1 and 1 by the activation function tanh and then multiplied by the output of the *sigmoid* neural network layer to obtain an output (Wang et al. 2020a):

$$o_t = \sigma(W_o[h_{t-1}, x_t] + b_o) \tag{6}$$

$$h_t = o_t \cdot \tanh(c_t) \tag{7}$$

where W_o represents the weight matrix and b_o represents the offset.

2.2.2 Convolutional neural network model

CNN is a kind of artificial neural network and its largest feature is weight sharing. Weight sharing can greatly reduce the number of weights, further reducing the complexity of the entire CNN. The CNN can directly accept images as an input and use filters to extract data features directly and automatically. Features do not require tedious and complicated manual design and the entire feature representation process is more automated (Yang et al. 2019a).

The CNN is composed of multiple network layers and each network layer has many independent neurons. The feature extraction filter performs a convolution operation on the input image and generate a feature map in the C1 layer after convolution. Next, neural network operation is carried out on feature map S1, including finding the weight between the two layers of neurons and adding the corresponding bias. Finally, a new feature mapping result S2 is obtained through the *sigmoid* function, which is a further abstraction of the C1 layer. This process is repeated until finally the result is input to a classifier to obtain an output (Akram et al. 2019).

2.2.3 Support vector machine model

The SVM is built based on statistical learning theory and has a solid theoretical foundation (Cortes and Vapnik 1995). The SVM has a good adaptability to practical problems such as high dimensionality, small samples, nonlinearity and local minima. This model is currently widely used in many fields, such as computers, ecology, medicine and engineering (Kwag et al. 2020). Based on the statistical learning theory, the SVM improves the generalization ability of the learning machine by seeking to minimize the structured risk, experience risk, and confidence range, so that the model can obtain higher accuracy even with a small number of samples (Moayedi et al. 2019).

The basic idea of SVM is as follows: when dealing with the linear indivisibility problem, the nonlinear problem in the original sample space is transformed into a linear problem in the high-dimensional feature space through a nonlinear transformation. Then, a constrained convex quadratic programming problem is solved in this new high-dimensional space, and the unique global optimal solution is obtained (Tinoco et al. 2018).

2.2.4 Random forest model

The random forest algorithm is a combination classification intelligent algorithm based on the statistical theory proposed by Breiman in 2001. It has a strong data mining capability and high prediction accuracy (Lin et al. 2018; Huang et al. 2022a).

The RF uses multiple classification trees to follow the ensemble learning rules. During its implementation, the prediction relationship is randomly changed to increase the diversity of the used forest tree species. The RF needs to manually specify the number of trees and that of variables for splitting nodes. The reliability of the model can only be guaranteed when parameter t is high enough. Since each tree is regarded as a completely independent random situation, the abundance of random trees can reduce the possibility of overfitting (Wongvibulsin et al. 2019).

2.3 Evaluation method of model accuracy

In addition to directly comparing the errors between the machine learning model predictions and the numerical simulation results, this study also introduces two quantitative statistics to evaluate the fitting effect of the model—root mean square error (RMSE) (Eq. (8)) and modelling efficiency (EF) (Eq. (9)) (Koopialipoor et al. 2018)—to compare the prediction accuracy of the four machine learning models.

$$\mathrm{RMSE} = \frac{\sqrt{\sum_{i=1}^{n} (y_i - \hat{y}_i)^2 / n}}{\bar{y}} * 100\% \tag{8}$$

where y_i represents the slope stability factor of each sample, $\hat{y}_i$ represents the predicted value of the machine learning modeling for each sample, and $\bar{y}$ represents an average value of the slope stability factor.

The RMSE value represents the percentage of a difference between the observed value y and the predicted value $\hat{y}$ relative to $\bar{y}$. Its magnitude reflects the relative error of the model used in fitting.

$$\mathrm{EF} = \left[\sum_{i=1}^{n} (y_i - \bar{y}_i)^2 - \sum_{i=1}^{n} (y_i - \hat{y}_i)^2 \right] / \sum_{i=1}^{n} (y_i - \bar{y}_i)^2 \tag{9}$$

The EF value is a standard statistical value for evaluating simulation accuracy. When $\sum_{i=1}^{n} (y_i - \hat{y}_i)^2 = 0$, EF reaches its maximum value of 1. The predicted $\hat{y}_i$ is in complete agreement with the observed y.

3 Construction of typical soil slopes

3.1 Overview of Ganzhou City

Ganzhou City is located in Jiangxi Province, China, with an area of 39,379.6 km^2. The natural environment of Ganzhou City is complex and it is one of the areas with more serious geological disasters. The terrain in Ganzhou City is different from east to west, with a trend of low altitude in the southwest and high altitude in the northeast. Most of the landforms are middle-low mountains and hilly areas, accounting for 75.62% of this city's total area. According to preliminary statistics, a total of 19,555 geological disasters occurred in Ganzhou City from 1998 to 2010, in which collapse and landslides were mainly distributed in the low mountain and hilly areas. The stratum lithology in this area is composed of metamorphic rock, granite, red clastic rock and general clastic rock, and is dominated by soil landslides. Debris flows are mostly developed in the middle and low mountain areas and areas prone to heavy rain, while karst collapses are distributed throughout Ganzhou City. Besides, the ground subsidence in the goaf is mainly distributed in the northern part of Ganzhou City. In general, the occurrence density of geological disasters in Ganzhou City is relatively high, with an average of 20 locations per 100 km^2.

3.2 Selection of control factors

The main factors affecting the slope stability are stratum lithology, geological structure, in situ stress, rock mass structure, water action, slope geometry and surface morphology. Among these influencing factors, the geometric influencing factors are mainly slope height and slope angles; the influencing factors of rock and the soil mechanics index refer to the volumetric weight, cohesion, internal friction angle and pore pressure ratio of rock and soil (Lu et al. 2020). Machine learning models are based on data mining and need to provide effective parameters for determination. Too many input parameters cause the stability analysis of the final expression irregular, and it is difficult to collect data. Too few parameters do not correctly reflect the slope stability content. After consulting the data (Kumar et al. 2014; Gordan et al. 2016; Zhou et al. 2019), the five control factors, the slope height, slope angle, cohesion, internal friction angle and volumetric weight are selected as the input variables of the machine learning models. The slope height (H) reflects the volume and weight of the slope, and the slope angle (α) is a key factor that generally governs the slope stability. Moreover, the cohesion (c) and internal friction angle (φ) are important mechanical indicators affecting soil strength. Finally, the volumetric weight (γ) reflects the grav–ity that promotes the occurrence of landslides.

3.3 Determination of control factors

In this study, the reasonable value range of each parameter is determined by analyzing the landslide data and geological data of Ganzhou City. The value range of H is 1–260 m, and the value range of α is 0°–44.5°. The value

ranges of c and φ are 23.3–56.8 kPa and 12.6°–51.7°, respectively. Besides, the value range of γ is 18.2–23.3 kN/m^3. Within the value range of each control factor, the value is selected based on interpolation. Considering that if the slope height and slope angle are set with too many kinds of values, it will be too complex to construct soil slope models. Hence, its most common situation is considered to select its values. The slope height is set to 65 m, 100 m, 135 m and 170 m. The slope angles are 20°, 25°, 30°, 35° and 40°. Because the value range of volumetric weight is small, three values are set to 18.2 kN/m^3, 19.7 kN/m^3 and 21.2 kN/m^3. For cohesion c and the internal friction angle φ, values are taken within the range of values with an interval of 5. The values of all control factors are shown in Table 1.

3.4 Construction of typical soil slope

Furthermore, the evolution characteristics of Ganzhou landslides are summarized, including the rock and soil mechanical indicators, thickness, slope length, slope height and slope angle (Yin et al. 2020). Most of the landslides in Ganzhou City are shallow landslides with a thickness ranging from 2 to 10 m, and the length of the slope is mostly within 40–200 m. Besides, the slope angle is generally between 15° and 40°. According to the evolution characteristics of these landslides, a series of typical accumulation layer slopes are constructed.

Based on these typical slopes, 20 types of slopes are established in the Geo-Studio software by setting different slope heights and slope angles (Table 1). Next, the three control factors of C, φ and γ are transformed and combined and then input to the established 20 types of slopes. This step adds rock and soil material properties to the slopes. As a result, a total of 2160 different soil slopes are obtained. Among them, the soil slope with a slope height of 100 m and a slope angle of 25° is selected as the sample, as shown in Fig. 4.

Table 1 Values setting rule of control factors

H (m)	α (°)	c (kPa)	φ (°)	γ (kN/m^3)
65	20	23.3	12.6	18.2
100	25	28.3	17.6	19.7
135	30	33.3	22.6	21.2
170	35	38.3	27.6	
	40	43.3	32.6	
		48.3	37.6	

4 Stability prediction of various soil slopes

4.1 Data acquisition

According to the values of the slope height, slope angle, cohesion, internal friction angle and volumetric weight determined in Sect. 3.3, a total of 2160 different slope models are constructed by perturbation and their combination. The slope stability factor is calculated by the limit equilibrium method in the Geo-Studio software. Each slope stability factor and its corresponding control factor is a slope sample, and the 2160 obtained groups of

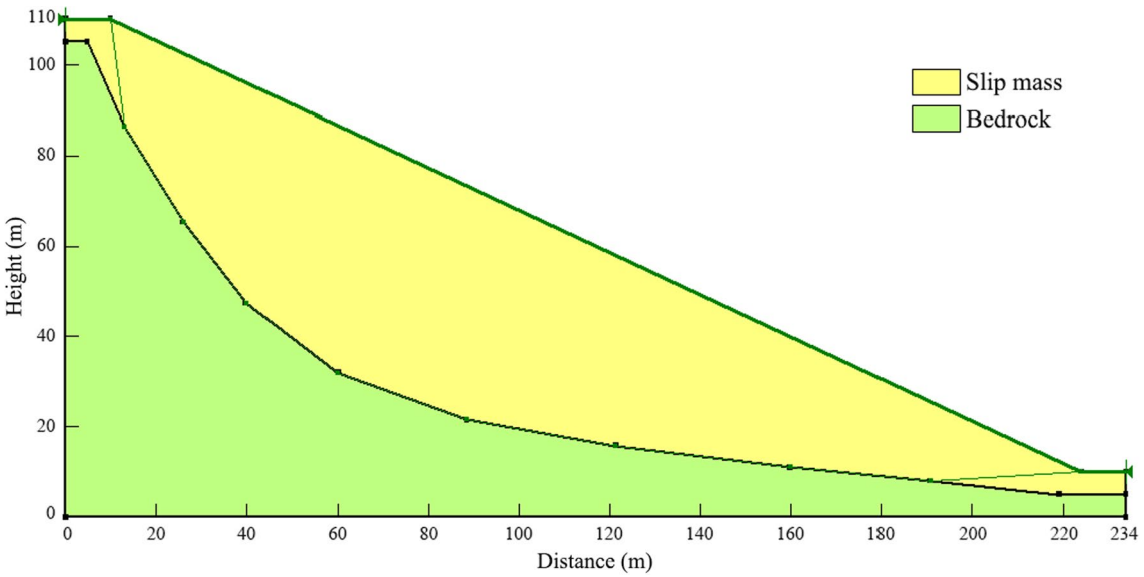

Fig. 4 A typical soil slope with slope height of 100 m and slope angle of 25°

slope sample data are used as the training sample data of the machine learning model. Similarly, according to the determined value range of slope stability control factors, the Excel 2016 software is used to randomly set three factor values for slope height and slope angle. Then nine different typical soil slopes are obtained by permutation and combination. After that, 50 groups of cohesion, internal friction angle and volumetric weight are randomly determined for each soil slope within the corresponding value range. A total of 450 soil slopes with different geotechnical mechanicals parameters are obtained. In the machine learning modelling, the 450 soil slopes and their control factors are the testing sample data.

The Geo-Studio software is used to calculate the slope stability factor of each soil slope through the limit equilibrium method (Jiang et al. 2017). The obtained slope stability factor is used as the actual slope stability factor of the slope, and is used for a comparison with the slope stability factors predicted by the machine learning models. Since there are 2160 sets of training sample data and 450 sets of prediction sample data, there are too many data to list them all. The seventy-two samples randomly selected from the training data are shown in Table 2, and 15 from the predicted data are shown in Table 3.

4.2 Machine learning model training

To obtain a more accurate prediction, the machine learning model needs to be trained before slope stability prediction to determine the optimal value of parameters in each machine learning model. For the SVM and RF (two traditional machine learning models), the training dataset is imported into SPSS modeler 18.0 software, and the optimal values of the required parameters in the SVM model and RF model are obtained by cross validation. In this study, the RBF is taken as the kernel function of the SVM model. After training the SVM model, the regularization parameter is set to 10, and the kernel function parameter Υ is set to 0.1. Additionally, by training the RF model, the number of decision trees constructed in the RF model is set to 10, the maximum number of nodes is set to 500, the maximum tree depth is set to 10 and the minimum child node size is set to 5.

For the LSTM and CNN (two deep learning models), there is no need to manually debug parameter values. When writing the deep learning algorithm, the training dataset and the testing dataset are marked with corresponding labels in the algorithm statement, and they are linked to the corresponding deep learning model. When the deep learning model starts to run, it conducts training through the linked training dataset and automatically searches for the optimal value of the parameters in the deep learning model.

4.3 Slope stability predictions from machine learning models

For the traditional machine learning models, the SVM model and the RF model, there is no need to adjust their parameters because they have been trained previously. The testing dataset is imported into the SPSS modeler 18.0 software and linked to the trained SVM model and RF model. After running, the corresponding dataset of slope stability factors is output. For the deep learning models, the CNN model and LSTM model, the corresponding labels are marked for the training dataset and testing dataset in the algorithm statement. The CNN and LSTM models search for the optimal values of the required parameters through the training data. After training the deep learning models, the slope stability is predicted directly with the testing dataset and the slope stability factor dataset is output.

After the slope stability prediction of 450 testing sample slopes, the prediction accuracy of the four machine learning models is evaluated by comparing the errors between the predicted values and the numerical simulation results and calculating the RMSE values and EF values of the four machine learning models. Because of the large quantity of data, 15 prediction samples are randomly selected from the all 450 samples and are shown in Table 4; the RMSE and EF values of each machine learning model are calculated using the all 450 samples. Table 4 shows that the slope stability factors predicted by the LSTM are close to the results of numerical simulation, and the absolute error of the randomly selected sample data is less than 0.05. Compared with that of other three machine learning models, the error of the slope stability prediction results of the LSTM model is smaller. Namely, the prediction accuracy of the LSTM model is higher.

According to Sect. 2.3, the smaller the RMSE value of the model or the closer the EF value of the model is to 1, the higher the prediction accuracy of the model is. Further information can be seen in Table 4. Figure 5 shows the RMSE value of the LSTM model is only 4.45%, which is the smallest among these of the four machine learning models. The EF value of the LSTM model is 0.9827, which is the closest to 1 among these for the four machine learning models. Therefore, the RMSE and EF values of the four machine learning models both suggest that the LSTM model has the highest slope stability prediction accuracy among all these models.

Table 2 Model training data sets

Sample number	c (kPa)	φ (°)	γ (kN/m^3)	H (m)	α (°)	Slope stability factor
1	33.3	17.6	18.2	65	30	1.003
2	23.3	12.6	19.7	65	30	0.689
3	28.3	12.6	19.7	65	30	0.731
4	33.3	32.6	19.7	65	30	1.696
5	48.3	32.6	19.7	65	30	1.819
6	38.3	37.6	19.7	65	30	2.028
7	23.3	12.6	21.2	65	30	0.675
8	43.3	32.6	21.2	65	30	1.753
9	33.3	22.6	18.2	65	35	1.127
10	38.3	12.6	19.7	65	35	0.749
11	43.3	27.6	19.7	65	35	1.401
12	43.3	37.6	19.7	65	35	1.913
13	33.3	17.6	18.2	65	40	0.815
14	48.3	17.6	18.2	65	40	0.918
15	23.3	22.6	18.2	65	40	0.926
16	43.3	22.6	18.2	65	40	1.067
17	38.3	17.6	19.7	65	40	0.830
18	23.3	37.6	19.7	65	40	1.551
19	43.3	32.6	21.2	65	40	1.425
20	43.3	37.6	21.2	65	40	1.661
21	28.3	12.6	19.7	100	25	0.786
22	23.3	37.6	19.7	100	25	2.316
23	23.3	32.6	19.7	100	30	1.560
24	33.3	17.6	18.2	100	35	0.789
25	43.3	27.6	18.2	100	35	1.240
26	28.3	32.6	18.2	100	40	1.286
27	48.3	27.6	19.7	100	40	1.154
28	23.3	37.6	21.2	100	40	1.485
29	28.3	22.6	18.2	135	25	1.257
30	23.3	37.6	18.2	135	25	2.205
31	23.3	17.6	21.2	135	25	0.952
32	38.3	32.6	21.2	135	25	1.887
33	43.3	32.6	21.2	135	25	1.905
34	38.3	12.6	18.2	135	30	0.672
35	28.3	22.6	21.2	135	30	1.067
36	23.3	27.6	21.2	135	30	1.300
37	23.3	12.6	18.2	135	35	0.546
38	28.3	17.6	18.2	135	35	0.758
39	33.3	17.6	21.2	135	35	0.759
40	43.3	22.6	18.2	135	40	0.893
41	28.3	37.6	19.7	135	40	1.466
42	43.3	12.6	18.2	170	25	0.769
43	33.3	32.6	18.2	170	25	1.888
44	33.3	22.6	19.7	170	25	1.260
45	48.3	22.6	21.2	170	25	1.297
46	23.3	37.6	21.2	170	25	2.205
47	33.3	27.6	18.2	170	30	1.325
48	43.3	32.6	18.2	170	30	1.628
49	23.3	12.6	19.7	170	30	0.589

Table 2 (continued)

Sample number	c (kPa)	φ (°)	γ (kN/m^3)	H (m)	α (°)	Slope stability factor
50	33.3	17.6	19.7	170	30	0.837
51	28.3	37.6	18.2	170	35	1.604
52	33.3	27.6	21.2	170	35	1.118
53	43.3	37.6	18.2	170	40	1.510
54	38.3	12.6	21.2	170	40	0.495
55	43.3	17.6	18.2	65	20	1.447
56	33.3	37.6	18.2	65	20	2.819
57	33.3	27.6	19.7	65	20	1.996
58	28.3	37.6	19.7	65	20	2.751
59	23.3	12.6	21.2	65	20	0.919
60	43.3	27.6	21.2	65	20	2.057
61	28.3	37.6	18.2	100	20	2.584
62	48.3	17.6	21.2	100	20	1.274
63	33.3	27.6	18.2	135	20	1.909
64	38.3	12.6	19.7	135	20	0.913
65	48.3	27.6	19.7	135	20	1.961
66	33.3	37.6	19.7	135	20	2.730
67	43.3	32.6	21.2	135	20	2.320
68	33.3	12.6	18.2	170	20	0.879
69	33.3	17.6	21.2	170	20	1.179
70	48.3	17.6	21.2	170	20	1.226
71	38.3	32.6	21.2	170	20	2.286
72	48.3	37.6	21.2	170	20	2.754

Table 3 Model testing data sets

Sample number	c (kPa)	φ (°)	γ (kN/m^3)	H (m)	α (°)	Slope stability factor
73	34.81	35.75	19.05	82	32	1.811
74	33.10	24.60	18.82	82	38	1.128
75	36.79	14.72	20.89	82	38	0.721
76	30.13	17.08	19.42	82	38	0.793
77	43.35	13.21	19.95	82	38	0.703
78	44.69	17.12	18.73	115	23	1.158
79	35.96	30.78	19.49	115	23	1.990
80	34.13	22.38	18.84	115	23	1.424
81	38.70	26.86	20.73	115	23	1.719
82	41.27	29.12	18.31	115	32	1.469
83	28.28	34.35	20.72	115	32	1.695
84	28.31	23.87	20.53	115	38	1.022
85	35.82	16.54	19.27	157	23	1.047
86	45.33	22.14	19.70	157	23	1.418
87	29.37	34.17	18.34	157	23	2.220

Table 4 Comparison of various model prediction results

Sample number	Numerical simulation results	SVM		RF		CNN		LSTM	
		Predicted value	Absolute error	Predicted value	Absolute error	Predicted value	Absolute error	Predicted value	Absolute error
73	1.811	1.813	0.002	1.695	−0.116	1.898	0.087	1.824	0.013
74	1.128	0.984	−0.144	1.149	0.021	1.049	−0.079	1.050	−0.078
75	0.721	0.613	−0.108	0.780	0.059	0.531	−0.190	0.716	−0.005
76	0.793	0.666	−0.127	0.713	−0.080	0.646	−0.147	0.755	−0.038
77	0.703	0.610	−0.093	0.768	0.065	0.529	−0.174	0.673	−0.030
78	1.158	1.164	0.006	1.047	−0.111	1.381	0.223	1.177	0.019
79	1.990	1.984	−0.006	1.925	−0.065	2.040	0.050	1.974	−0.016
80	1.424	1.415	−0.009	1.267	−0.157	1.590	0.166	1.375	−0.049
81	1.719	1.715	−0.004	1.655	−0.064	1.832	0.113	1.722	0.003
82	1.469	1.434	−0.035	1.429	−0.040	1.433	−0.036	1.420	−0.049
83	1.695	1.644	−0.051	1.628	−0.067	1.659	−0.036	1.638	−0.057
84	1.022	0.859	−0.163	1.068	0.046	0.867	−0.155	0.922	−0.100
85	1.047	1.033	−0.014	1.014	−0.033	1.250	0.203	1.088	0.041
86	1.418	1.415	−0.003	1.294	−0.124	1.592	0.174	1.410	−0.008
87	2.220	2.183	−0.037	2.193	−0.027	2.191	−0.029	2.128	−0.092
RMSE value		6.26%		7.77%		10.11%		4.45%	
EF value		0.9696		0.9435		0.9301		0.9827	

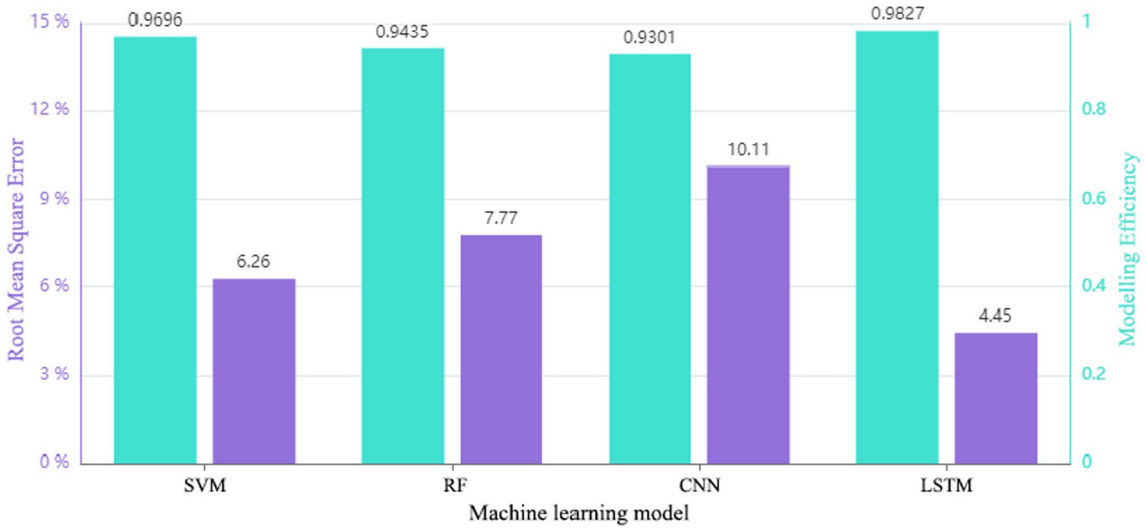

Fig. 5 Comparison of various model predictions

5 Discussion

5.1 Innovations of this study

(1) Deep learning has been widely used in other fields. However, it has rarely been used for slope stability prediction. In other words, the current relevant studies rely on the traditional machine learning models. In particular, the LSTM model of deep learning was innovatively proposed in this study for slope stability prediction. Through comparative studies with the CNN, SVM and RF models, the feasibility and high precision of the LSTM model were revealed.

(2) The slope used in this study is a generalized soil slope based on a large number of actual slope statistics. Considering the five control factors having great influence on the slope stability, a large number of practical slope models were constructed. Furthermore, by changing the value of each control factor, 2160 slopes were constructed to form the slope knowledge base. The machine learning models were trained through the slope knowledge base to realize a rapid and accurate prediction of the slope stability of any slope within the value ranges of the five control factors.
(3) Existing studies often only build machine learning models for dozens of slopes. However, machine learning is more suitable for predicting samples with a large quantity of data, and an excessively small quantity of data will lead to a great uncertainty in machine learning modelling. In this study, there are 2160 training data samples and 450 prediction samples. The quantity of data is far greater than that in previous studies, which can effectively reduce the modelling uncertainty.
(4) In this study, the testing sample data were obtained randomly within the value ranges of the five control factors, and the number was large enough to be sufficiently representative of the possible slopes within the value ranges. If subsequent work or other scholars need to predict the stability of a single slope in the area, the values of the five control factors of a single slope can be input into the LSTM model, and the slope stability factor will be output.

5.2 Existing deficiencies and the future improvement

(1) In this study, five control factors affecting slope stability were considered as the input variables of machine learning models. These five control factors all belong to the nature of the slope. However, the occurrence of landslides is usually activated by external inducing factors in addition to the slope's controlling factors. In subsequent studies, external inducers such as rainfall and slope cutting can be added to the input variables of the machine learning model to realize real-time and accurate prediction of the slope stability under external inducer conditions.
(2) The soil slope in this study is a two-dimensional slope model established by the Geo-Studio software, while the slope in real life is a three-dimensional entity. The two-dimensional soil slope is a simplified treatment of the slope and does not consider the influence of slope width on its stability. In the next study, a three-dimensional soil slope can be considered for slope stability prediction. In the current research, the efficiency of 3D slope stability based on numerical simulation is low. Using machine learning instead of numerical simulation to calculate slope stability can greatly improve the efficiency of slope stability prediction when ensuring accuracy.
(3) In this study, slope stability factors obtained by the limit equilibrium method were compared with the predictions of the four machine learning models to analyze the prediction accuracy of the four machine learning models. However, the slope stability factor calculated by the limit equilibrium method is only a predicted value, which is not equal to the real value of the slope stability factor. In future study, it will be worth considering whether the data that are closer to the real value of the slope stability factor can be found for comparison with the predicted results of the machine learning models.

6 Conclusions

In this paper, there were 2160 training sample slopes and 450 prediction sample slopes. The data volume of the sample slopes was much larger than that of the previous studies, and it was representative enough for all the slopes in the study area. The machine learning models were trained through the training sample data. Then the prediction sample data were input into the trained machine learning to predict slope stability. Four machine learning models were adopted, of which the LSTM and CNN were deep learning models and the SVM and RF were traditional machine learning models. The four machine learning models used the same data for a slope stability prediction and evaluated the model prediction accuracy by calculating the RMSE and EF values of their predictions.

According to the evaluation of the predictions of the four machine learning models in Sect. 4.3, the slope stability factor of each sample slope predicted by the LSTM model was closer to that calculated by the limit equilibrium method. The RMSE and EF values of the four machine learning models were calculated, showing the same trend. That is, the prediction accuracy of the LSTM model was the highest, followed by the SVM, RF and CNN models from high to low. It can be concluded that the LSTM model has a great feasibility in slope stability prediction, and a higher prediction accuracy can be obtained through LSTM than the above traditional machine learning models.

Acknowledgements This research is funded by the National Natural Science Foundation of China (41807285)

Declarations

Conflict of interest The authors declare that they have no conflict of interest.

References

Abdalla JA, Attom MF, Hawileh R (2014) Prediction of minimum factor of safety against slope failure in clayey soils using artificial neural network. Environ Earth Sci 73:5463–5477. https://doi.org/10.1007/s12665-014-3800-x

Akram MW, Li G, Jin Y, Chen X, Zhu C, Zhao X, Khaliq A, Faheem M, Ahmad A (2019) CNN based automatic detection of photovoltaic cell defects in electroluminescence images. Energy 189:116319. https://doi.org/10.1016/j.energy.2019.116319

Amin J, Sharif M, Raza M, Saba T, Sial R, Shad SA (2019) Brain tumor detection: a long short-term memory (LSTM)-based learning model. Neural Comput Appl 32:15965–15973. https://doi.org/10.1007/s00521-019-04650-7

Bui D, Moayedi H, Gör M, Jaafari A, Foong LK (2019) Predicting slope stability failure through machine learning paradigms. ISPRS Int J Geo-Inf 8:395. https://doi.org/10.3390/ijgi8090395

Chang Z, Catani F, Huang F, Liu G, Meena SR, Huang J, Zhou C (2022) Landslide susceptibility prediction using slope unit-based machine learning models considering the heterogeneity of conditioning factors. J Rock Mech Geotech Eng. https://doi.org/10.1016/j.jrmge.2022.07.009

Chen Y, Cui S, Chen P, Yuan Q, Kang P, Zhu L (2021) An LSTM-based neural network method of particulate pollution forecast in China. Environ Res Lett 16:044006. https://doi.org/10.1088/1748-9326/abe1f5

Cortes C, Vapnik V (1995) support-vector networks. Mach Learn 20:273–297. https://doi.org/10.1023/a:1022627411411

Criss RE, Yao WM, Li CD, Tang HM (2020) A predictive, two-parameter model for the movement of reservoir landslides. J Earth Sci 31:1051–1057. https://doi.org/10.1007/s12583-020-1331-9

Dai C, Li WL, Wang D, Lu HY, Xu Q, Jian J (2021) Active landslide detection based on sentinel-1 data and InSAR technology in Zhouqu county, Gansu Province, Northwest China. J Earth Sci 32:1092–1103. https://doi.org/10.1007/s12583-020-1380-0

Gao W, Raftari M, Rashid ASA, Mu'azu MA, Jusoh WAW (2019) A predictive model based on an optimized ANN combined with ICA for predicting the stability of slopes. Eng Comput 36:325–344. https://doi.org/10.1007/s00366-019-00702-7

Gordan B, Armaghani DJ, Hajihassani M, Monjezi M (2016) Prediction of seismic slope stability through combination of particle swarm optimization and neural network. Eng Comput 32:85–97. https://doi.org/10.1007/s00366-015-0400-7

He XL, Xu C, Qi WW, Huang YD, Cheng J, Xu XW, Yao Q, Lu YK, Dai BY (2021) Landslides triggered by the 2020 Qiaojia M(w)5.1 earthquake, Yunnan, China: distribution, influence factors and tectonic significance. J Earth Sci 32:1056–1068. https://doi.org/10.1007/s12583-021-1492-1

Huang F, Yin K, He T, Zhou C, Zhang J (2016) Influencing factor analysis and displacement prediction in reservoir landslides: a case study of Three Gorges Reservoir (China). Tehnički Vjesnik 23:617–626

Huang F, Cao Z, Jiang S-H, Zhou C, Huang J, Guo Z (2020a) Landslide susceptibility prediction based on a semi-supervised multiple-layer perceptron model. Landslides 17:2919–2930

Huang F, Yang J, Zhang B, Li Y, Huang J, Chen N (2020b) Regional terrain complexity assessment based on principal component analysis and geographic information system: a case of Jiangxi Province, China. ISPRS Int J Geo-Inf 9:539

Huang YD, Xu C, Zhang XL, Xue CJ, Wang SY (2021) An updated database and spatial distribution of landslides triggered by the Milin, Tibet M(w)6.4 earthquake of 18 November 2017. J Earth Sci 32:1069–1078. https://doi.org/10.1007/s12583-021-1433-z

Huang F, Chen J, Liu W, Huang J, Hong H, Chen W (2022a) Regional rainfall-induced landslide hazard warning based on landslide susceptibility mapping and a critical rainfall threshold. Geomorphology. https://doi.org/10.1016/j.geomorph.2022.108236

Huang F, Tao S, Li D, Lian Z, Catani F, Huang J, Li K, Zhang C (2022b) Landslide susceptibility prediction considering neighborhood characteristics of landslide spatial datasets and hydrological slope units using remote sensing and GIS technologies. Rem Sens 14:4436

Jiang SH, Huang JS, Yao C, Yang JH (2017) Quantitative risk assessment of slope failure in 2-D spatially variable soils by limit equilibrium method. Appl Math Model 47:710–725. https://doi.org/10.1016/j.apm.2017.03.048

Jiang JY, Zhang ZW, Wang D, Wang LG, Han XP (2022) Web pillar stability in open-pit highwall mining. Int J Coal Sci Technol 9(1):12. https://doi.org/10.1007/s40789-022-00483-3

Kang F, Xu B, Li J, Zhao S (2017) Slope stability evaluation using Gaussian processes with various covariance functions. Appl Soft Comput 60:387–396. https://doi.org/10.1016/j.asoc.2017.07.011

Koopialipoor M, Jahed Armaghani D, Hedayat A, Marto A, Gordan B (2018) Applying various hybrid intelligent systems to evaluate and predict slope stability under static and dynamic conditions. Soft Comput 23:5913–5929. https://doi.org/10.1007/s00500-018-3253-3

Kumar S, Basudhar PK (2018) A neural network model for slope stability computations. Géotechnique Letters 8:149–154. https://doi.org/10.1680/jgele.18.00022

Kumar M, Samui P, Naithani AK (2014) Determination of stability of epimetamorphic rock slope using minimax probability machine. Geomat Nat Haz Risk 7:186–193. https://doi.org/10.1080/19475705.2014.883440

Kwag S, Hahm D, Kim M, Eem S (2020) Development of a probabilistic seismic performance assessment model of slope using machine learning methods. Sustainability. https://doi.org/10.3390/su12083269

Li W, Shi Y, Huang F, Hong H, Song G (2021) Uncertainties of collapse susceptibility prediction based on remote sensing and GIS: effects of different machine learning models. Front Earth Sci. https://doi.org/10.3389/feart.2021.731058

Liang H, Sun X, Sun Y, Gao Y (2017) Text feature extraction based on deep learning: a review. EURASIP J Wirel Commun Netw 2017:211. https://doi.org/10.1186/s13638-017-0993-1

Lin Y, Zhou K, Li J (2018) Prediction of slope stability using four supervised learning methods. IEEE Access 6:31169–31179. https://doi.org/10.1109/access.2018.2843787

Liu H, Mi X-W, Li Y-F (2018) Wind speed forecasting method based on deep learning strategy using empirical wavelet transform, long short term memory neural network and Elman neural network.

Energy Convers Manage 156:498–514. https://doi.org/10.1016/j.enconman.2017.11.053

Lu R, Wei W, Shang K, Jing X, Tang ZC (2020) Stability analysis of jointed rock slope by strength reduction technique considering ubiquitous joint model. Adv Civil Eng 2020:1–13. https://doi.org/10.1155/2020/8862243

Moayedi H, Bui D, Kalantar D, Foong L (2019) Machine-learning-based classification approaches toward recognizing slope stability failure. Appl Sci 9:4638. https://doi.org/10.3390/app9214638

Palenzuela Baena JA, Scifoni S, Marsella M, De Astis G, Irigaray Fernández C (2019) Landslide susceptibility mapping on the islands of Vulcano and Lipari (Aeolian Archipelago, Italy), using a multi-classification approach on conditioning factors and a modified GIS matrix method for areas lacking in a landslide inventory. Landslides 16:969–982. https://doi.org/10.1007/s10346-019-01148-0

Qi C, Tang X (2018) A hybrid ensemble method for improved prediction of slope stability. Int J Numer Anal Meth Geomech 42:1823–1839. https://doi.org/10.1002/nag.2834

Qian ZG, Li AJ, Chen WC, Lyamin AV, Jiang JC (2019) An artificial neural network approach to inhomogeneous soil slope stability predictions based on limit analysis methods. Soils Found 59:556–569. https://doi.org/10.1016/j.sandf.2018.10.008

Ray A, Kumar V, Kumar A, Rai R, Khandelwal M, Singh TN (2020) Stability prediction of Himalayan residual soil slope using artificial neural network. Nat Hazards 103:3523–3540. https://doi.org/10.1007/s11069-020-04141-2

Rukhaiyar S, Alam MN, Samadhiya NK (2017) A PSO-ANN hybrid model for predicting factor of safety of slope. Int J Geotech Eng. https://doi.org/10.1080/19386362.2017.1305652

Schmidhuber J (2015) Deep learning in neural networks: an overview. Neural Netw 61:85–117. https://doi.org/10.1016/j.neunet.2014.09.003

Selvaraju RR, Cogswell M, Das A, Vedantam R, Parikh D, Batra D (2020) Grad-CAM: visual explanations from deep networks via gradient-based localization. Int J Comput Vision 128:336–359. https://doi.org/10.1007/s11263-019-01228-7

Sun DL, Xu JH, Wen HJ, Wang Y (2020) An optimized random forest model and its generalization ability in landslide susceptibility mapping: application in two areas of Three Gorges Reservoir, China. J Earth Sci 31:1068–1086. https://doi.org/10.1007/s12583-020-1072-9

Tan F, Yu J, Jiao YY, Lin DW, Lv JH, Cheng Y (2021) Rapid assessment of landslide risk level based on deep learning. Arab J Geosci 14:220. https://doi.org/10.1007/s12517-021-06616-3

Tian Y, Zhang K, Li J, Lin X, Yang B (2018) LSTM-based traffic flow prediction with missing data. Neurocomputing 318:297–305. https://doi.org/10.1016/j.neucom.2018.08.067

Tinoco J, Gomes Correia A, Cortez P, Toll DG (2018) Stability condition identification of rock and soil cutting slopes based on soft computing. J Comput Civ Eng 32:04017088. https://doi.org/10.1061/(asce)cp.1943-5487.0000739

Wang P, Jiang A, Liu X, Shang J, Zhang L (2018) LSTM-based EEG classification in motor imagery tasks. IEEE Trans Neural Syst Rehabil Eng 26:2086–2095. https://doi.org/10.1109/TNSRE.2018.2876129

Wang L, Xu X, Gui R, Yang R, Pu F (2020a) Learning rotation domain deep mutual information using convolutional LSTM for unsupervised PolSAR image classification. Rem Sens 12:4075. https://doi.org/10.3390/rs12244075

Wang P, Wang S, Zhu C, Zhang Z (2020b) Classification and extent determination of rock slope using deep learning. Geomech Geophys Geo-Energy Geo-Resour 6:33. https://doi.org/10.1007/s40948-020-00154-0

Wongvibulsin S, Wu KC, Zeger SL (2019) Clinical risk prediction with random forests for survival, longitudinal, and multivariate (RF-SLAM) data analysis. BMC Med Res Methodol 20:1. https://doi.org/10.1186/s12874-019-0863-0

Wu H, Fang WZ, Kang Q, Tao WQ, Qiao R (2019) Predicting effective diffusivity of porous media from images by deep learning. Sci Rep 9:20387. https://doi.org/10.1038/s41598-019-56309-x

Wu HS, Chen YL, Lv HY, Xie QH, Chen YG, Gu J (2022) Stability analysis of rib pillars in highwall mining under dynamic and static loads in open-pit coal mine. Int J Coal Sci Technol 9(1):38. https://doi.org/10.1007/s40789-022-00504-1

Xie P, Zhou A, Chai B (2019) The application of long short-term memory(LSTM) method on displacement prediction of multifactor-induced landslides. IEEE Access 7:54305–54311. https://doi.org/10.1109/access.2019.2912419

Yang D, Zhang J, Wang S, Zhang X (2019a) A time-aware CNN-based personalized recommender system. Complexity 2019:1–11. https://doi.org/10.1155/2019/9476981

Yang Y, Sun Y, Sun G, Zheng H (2019b) Sequential excavation analysis of soil-rock-mixture slopes using an improved numerical manifold method with multiple layers of mathematical cover systems. Eng Geol 261:105278. https://doi.org/10.1016/j.enggeo.2019.105278

Yang Y, Wu W, Zheng H (2020) Stability analysis of slopes using the vector sum numerical manifold method. Bull Eng Geol Env 80:345–352. https://doi.org/10.1007/s10064-020-01903-x

Yao X, Moon SK, Bi G (2017) A hybrid machine learning approach for additive manufacturing design feature recommendation. Rapid Prototyp J 23:983–997. https://doi.org/10.1108/rpj-03-2016-0041

Yin X, Lin H, Chen Y, Wang Y, Zhao Y (2020) Precise evaluation method for the stability analysis of multi-scale slopes. Simulation 96:841–848. https://doi.org/10.1177/0037549720943274

Zhang W, Goh ATC (2016) Multivariate adaptive regression splines and neural network models for prediction of pile drivability. Geosci Front 7:45–52. https://doi.org/10.1016/j.gsf.2014.10.003

Zhao H, Deng K, Li N, Wang Z, Wei W (2020) Hierarchical spatial-spectral feature extraction with long short term memory (LSTM) for mineral identification using hyperspectral imagery. Sensors (basel) 20:6854. https://doi.org/10.3390/s20236854

Zhou D-X (2018) Deep distributed convolutional neural networks: Universality. Anal Appl 16:895–919. https://doi.org/10.1142/s0219530518500124

Zhou J, Li EM, Yang S, Wang MZ, Shi XZ, Yao S, Mitri HS (2019) Slope stability prediction for circular mode failure using gradient boosting machine approach based on an updated database of case histories. Saf Sci 118:505–518. https://doi.org/10.1016/j.ssci.2019.05.046